

The intermediate age open cluster NGC 2660^{*}

S. Sandrelli^{1,2}, A. Bragaglia¹, M. Tosi¹, G. Marconi³

¹ Osservatorio Astronomico di Bologna, Via Ranzani 1, I-40127 Bologna, Italy, e-mail sandrelli, angela, tosi @bo.astro.it

² Osservatorio Astronomico di Brera, Via Brera 28, I-20121 Milano, Italy, e-mail stefano@brera.mi.astro.it

³ Osservatorio Astronomico Roma, Via dell'Osservatorio 5, I-00040 Monte Porzio, Italy, e-mail marconi@coma.mporzio.astro.it

ABSTRACT

We present CCD UBVI photometry of the intermediate old open cluster NGC2660, covering from the red giants region to about seven magnitudes below the main sequence turn-off.

Using the synthetic Colour - Magnitude Diagram method, we estimate in a self-consistent way values for distance modulus ($(m-M)_0 \simeq 12.2$), reddening ($E(B - V) \simeq 0.40$), metallicity ($[Fe/H]$ about solar), and age ($\tau \lesssim 1$ Gyr). A 30% population of binary stars turns out to be probably present.

Key words: Open clusters and associations: general – open clusters and associations: individual: NGC2660 – Hertzsprung-Russell (HR) diagram

1 INTRODUCTION

Galactic open clusters cover a large range of distances, metallicities and ages, which allows us to map out the disc of our Galaxy, so that they reveal themselves to be a precious tool in the study of the chemical and dynamical evolution of the Milky Way.

We have undertaken a program to carefully analyse open clusters at various positions, metallicities and ages. Our homogeneous analyses are addressed mostly to the older objects (i.e. with ages larger than the Hyades).

Distance, age, reddening and approximate metallicity of the clusters are derived from comparison of the observed colour-magnitude diagrams (CMDs) to synthetic ones generated by a numerical code based on stellar evolution tracks and taking into account theoretical and observational uncertainties (Tosi et al. 1991). This method, alternative to the classical isochrone fitting, has proven much more powerful and successful in studying the evolutionary status and properties of the analysed objects. We have already applied it to several Galactic open clusters, namely: NGC7790 (Romeo et al. 1989), NGC2243 (Bonifazi et al. 1990), Cr261 (Gozzoli et al. 1996), NGC6253 (Bragaglia et al. 1997), NGC2506 (Marconi et al. 1997), and Berkeley 21 (Tosi et al. 1998).

NGC2660 is an intermediate age open cluster located at coordinates RA(2000) = 8:42:18, DEC(2000) = -47:09, and $l_{II} = 266^\circ$, $b_{II} = -3.0^\circ$. In the past it has also been studied because of a carbon star possibly associated to it (GV Vel, e.g. Hartwick & Hesser 1973, and recently Groenewegen, van den Hoeck & de Jong 1995).

The cluster CMD has already been published by

Hartwick & Hesser (1973, hereafter HH73), and by Frandsen, Dreyer & Kjeldsen (1989, hereafter FDK), but our new data reach fainter and/or have higher photometric precision. HH73 employed photoelectric U, B, V , photographic B, V , and photoelectric $wbyH_\beta$ measures to determine the following properties: $E(B - V) \simeq 0.38$, $(m-M)_0 = 12.3 \pm 0.3$, age ~ 1.2 Gyr, metallicity similar to the Hyades, and high probability of membership for the N-type carbon star. FDK studied several open clusters to find trace of stellar activity and variability, using repeated Johnson V and Gunn r photometry on a period of a few days (4 to 12, depending on the cluster). In NGC2660 they found many candidate variables (about 10% of the stars measured on a 2×3 arcmin² field). They argue that the cluster has a normal number of δ -Scuti variables, and many low amplitude variables, both on the main sequence (MS) and in the giant region. They present V and r light curves for three objects, one of which looks unquestionably a variable (defined as a rotating spotted K-type star), and two *may* be badly sampled eclipsing variables.

The cluster metallicity has been measured by various authors, but with inconsistent results. HH73 estimated the metallicity to be $\leq [Fe/H]_{Hyades}$ on the basis of the ultraviolet excess in the two-colour diagram of four red giant stars. Hesser & Smith (1987), employing DDO photometry of 13 giant stars, determined a metallicity 0.6 dex lower than in the Hyades, or $[Fe/H] = -0.4$, on a scale where $[Fe/H]_{Hyades} = +0.2$. Geisler, Clariá & Minniti (1992), using Washington photometry on cluster giants, investigated the metallicity of several open clusters with an accuracy of about 0.2 dex. While in most cases their metallicities show good agreement with other determinations, NGC2660 is an exception, with $[Fe/H] = -1.05 \pm 0.16$. They also claim that

^{*} Based on observations made in La Silla, ESO

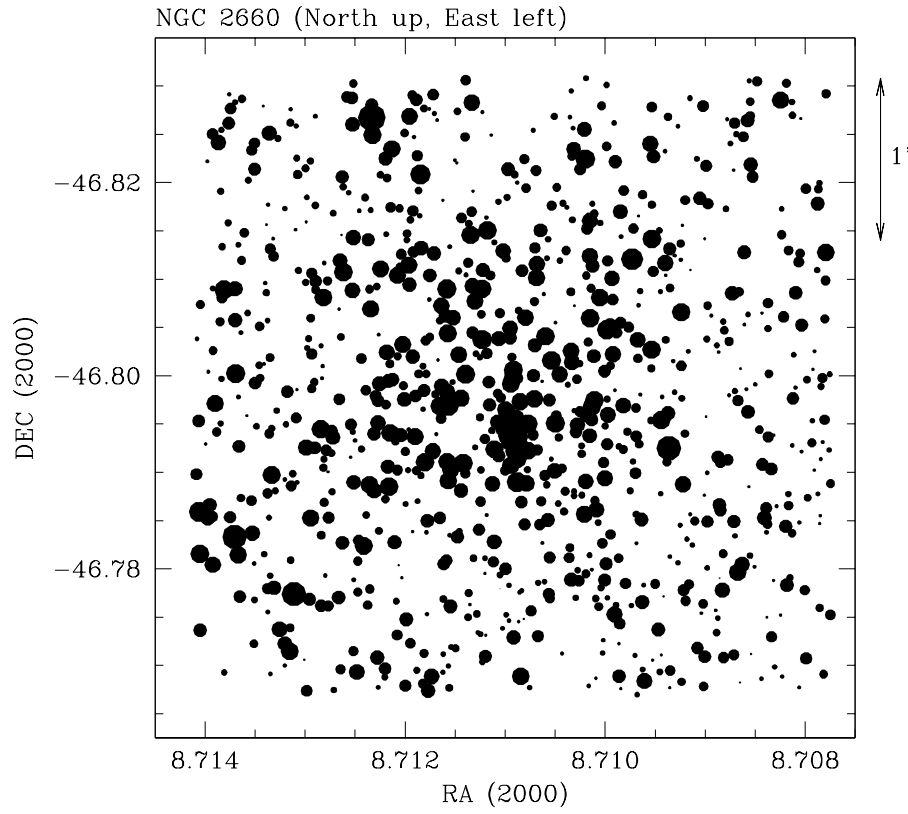


Figure 1. Map of the observed field derived from the photometry of one of the deep V frames: the bright carbon star, and a few saturated field stars are missing. North is up and East left; the field is 3.8×3.8 arcmin².

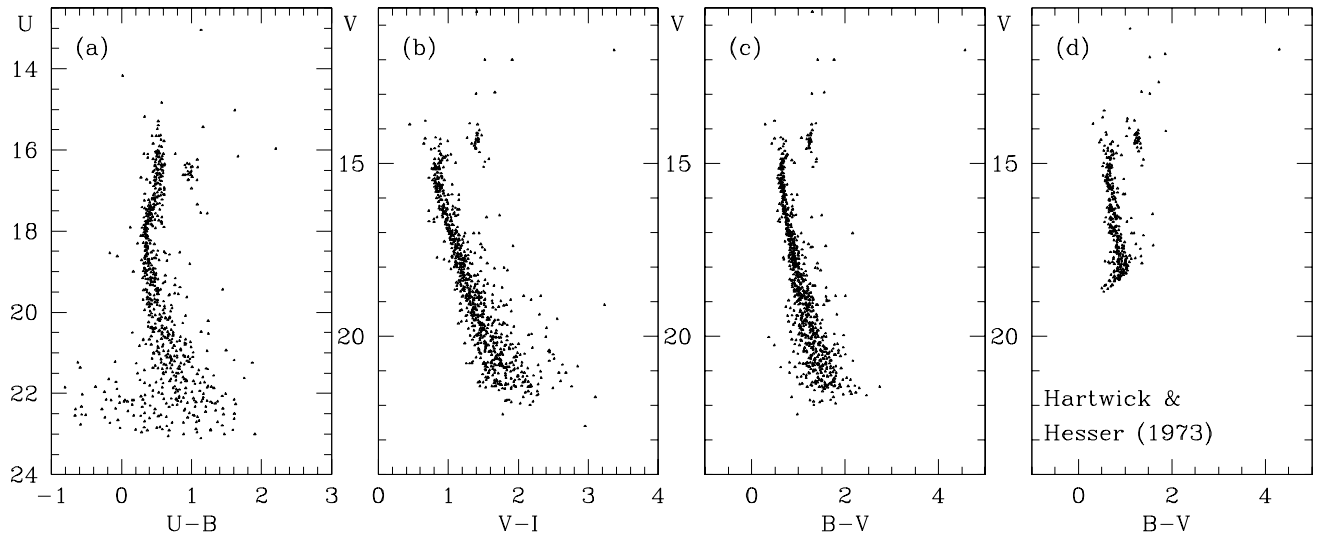


Figure 2. (a,b,c) Colour Magnitude Diagrams for our sample, and (d) comparison with HH73

the Houdashelt, Frogel & Cohen (1992) IR observations of the cluster go in the same direction, resulting in a CMD indicative of a quite metal-poor population. Friel (1995) cites for NGC2660 a value of $[\text{Fe}/\text{H}]=+0.06$, taken from Lyngå (1987); there are no spectroscopic measures for this cluster made by her group. The last determination comes again from DDO photometry, but with a new abundance calibration, and is found in Piatti, Clariá & Geisler (1995): they obtain $[\text{Fe}/\text{H}]=-0.27\pm 0.13$ on 5 stars with membership information.

On the contrary, the reddening values have always been found in good agreement. HH73 give $E(B-V)=0.38\pm 0.05$, from a variety of methods, comprising the position of MS stars in the two-colour diagram, a few nearby Cepheids, and Strömgren colours. Hesser & Smith (1987) infer a value of $E(B-V)=0.35\pm 0.03$ from their DDO photometry. Lewis & Freeman (1989) compute, from their reddening model based on observations of old disc giants, $E(B-V)=0.38$.

As to the age of NGC2660, HH73 determined a value of ~ 1.2 Gyr using isochrones computed by them on purpose. Lyngå (1987) cites 1.6 Gyr. Janes & Phelps (1994), on the basis of the δV method, compute an age of 0.9 Gyr, while Carraro & Chiosi (1994) and Carraro, Ng & Portinari (1998) derive 0.7 Gyr (adopting $[\text{Fe}/\text{H}]=+0.06$).

In Section 2 we describe the observations and data analysis; in Section 3 we present the derived CMDs involving $UBVI$ photometry and discuss the presence of binary stars. In Section 4 we compare observed and synthetic CMDs and derive metallicity, age, distance and reddening. Finally, the conclusions will be reviewed in Section 5.

2 OBSERVATION AND DATA REDUCTIONS

NGC2660 was observed at the 0.91m Dutch telescope located in La Silla, Chile, on May 8, 1997; the field was centered on the cluster, at coordinates $\text{RA}(2000)=8:42:36$, $\text{DEC}(2000)=-47:13:25$. The direct camera mounted the CCD #33, a Tek 512 \times 512, with a scale of 0.442 arcsec/pix, yielding a field of view of 3.8 \times 3.8 arcmin². The observed region is shown in Fig. 1, derived from our photometry (bright objects, like the carbon star, and a few field stars, are missing), and oriented with North up and East left.

Observations were done in the Bessel U, B, V filters (ESO # 634, 419, 420) and Gunn i (ESO # 465). Exposures in B, V, i were both short (30 or 60 seconds) and long (10 or 15 minutes). The single 30 minutes U exposure doesn't reach as faint as the other bands, but is useful for reddening determination, true cluster members selection and binary stars detection.

The observations were performed on a photometric night, with standard stars fields observed before and after the cluster. The airmass was always less than 1.5, and seeing conditions were quite poor, but this did not pose any problem even in the (relatively) crowded central region: no star was lost due to confusion with a nearby object. The seeing values for the four images used as master frames for the reduction are indicated in Table 1.

Standard CCD reductions of bias and dark current subtraction, trimming, and flatfield correction were performed.

The sum of two deep frames (300 and 900 seconds) in V has been used to search for stellar objects, setting the

Table 1. Aperture correction, airmass and extinction coefficients for the instrumental magnitudes of the four reference frames in the U, B, V and I filters. The fifth column gives the corresponding seeing values.

Filter	aperture (mag)	airmass	extinction (k_λ)	seeing (arcsec)
U	-0.233	1.17	0.59	1.64
B	-0.252	1.43	0.22	2.00
V	-0.315	1.11	0.12	1.30
I	-0.361	1.21	0.06	1.28

minimum photometric threshold for object detection at 3σ above the local sky background. The stars which seemed to be saturated were recovered on a V frame of shorter exposure (30 seconds). All the identified objects were then fitted in all the others frames.

We applied to all frames the usual procedure for PSF study and fitting available in DAOPHOT-II (Stetson 1992) in IRAF[†] environment.

For every filter, we identified a reference frame which we used to calibrate the PSF derived magnitudes of any other images. We chose 15-20 isolated stars in all the four reference images and computed the aperture corrections to the PSF estimates. In a given filter, the measured magnitude m is obtained as

$$m = m_{psf} + A - k \cdot F_z$$

where m_{psf} is the PSF derived magnitudes, A the aperture correction, k the extinction coefficient for that filter and F_z the airmass (Table 1).

2.1 Photometric calibrations

The conversion from instrumental magnitudes to the Johnson-Cousins standard system was obtained using the following set of primary calibrators: PG0918+019, PG1323-086, PG1525-071, Mark A (Landolt 1992). The adopted stars span a wide range in colour ($-0.27 \leq B-V \leq 1.13$), and cover almost the whole interval of interest for this cluster, from the MS Turn-Off (TO) point to (with a small extrapolation) the red clump. Standard stars fields were analysed using aperture photometry. The calibration equations were derived using La Silla mean extinction coefficients for the month of May, taken from the database maintained by the the Geneva Observatory photometric group.

We obtained equations in the form:

$$U(u, u-b) = u + 0.039(\pm 0.003) \cdot (u-b) - 5.235(\pm 0.01)$$

$$B(b, b-v) = b + 0.069(\pm 0.001) \cdot (b-v) - 3.347(\pm 0.001)$$

$$V(v, b-v) = v + 0.008(\pm 0.010) \cdot (b-v) - 2.952(\pm 0.02)$$

$$V(v, v-i) = v + 0.098(\pm 0.010) \cdot (v-i) - 2.946(\pm 0.001)$$

$$I(i, v-i) = i - 0.043(\pm 0.005) \cdot (v-i) - 4.075(\pm 0.001)$$

[†] IRAF is distributed by the NOAO, which are operated by AURA, under contract with NSF

Table 2. Completeness of our measurements. Each value is the average of 10 to 30 trials for $U, B, V,$ and I .

Mag interval	%U	%B	%V	%I
13.0				100
13.5				94
14.0		100		94
14.5		90	100	94
15.0		98	98	83
15.5		90	98	87
16.0	100	97	100	85
16.5	96	82	96	78
17.0	98	100	98	71
17.5	100	95	88	64
18.0	97	97	95	57
18.5	100	92	91	40
19.0	95	93	87	10
19.5	96	90	84	20
20.0	92	80	76	< 10
20.5	92	70	79	
21.0	78	61	64	
21.5	74	47	52	
22.0	52	45	37	
22.5	31	22	10	
23.0	20	10	< 10	
23.5	< 10	< 10		

where u, b, v, i are instrumental magnitudes, and U, B, V, I are the corresponding Johnson-Cousins magnitudes.

2.2 Completeness analysis

A suitable new IRAF task (ALLBIN) was prepared to test automatically the completeness of our luminosity function in the U, B, V and I band. In short, ALLBIN uses the routine ADDSTAR (in DAOPHOT-II) to add to the original deepest frames in each filter a pattern of artificial stars, distributed in colour as the real ones ($\simeq 10\%$ of the total in each magnitude bin), at random positions. The obtained “artificial frames” were then reduced using exactly the same procedure and the same PSF used for the original images.

We considered as “recovered” only those stars found in their given position and magnitude bin. The completeness was then derived as the ratio $N_{recovered}/N_{added}$ of the artificial stars generated.

We performed 10 to 30 trials per bin in every band, depending on the stability of the results. The final averaged results are reported in Table 2.

3 THE COLOUR-MAGNITUDE DIAGRAMS

The stars measured in our field are 866; the corresponding CMDs are shown in Fig. 2, together with the older data by HH73. The cluster MS is well delineated, and can be followed for about 7 magnitudes fainter than the TO. There is a well populated clump of red stars, which is attributable to the core-He burning phase, and a few red giants are also visible.

The carbon star, #188 in our numbering system, is visible at $U = 19.48, B = 16.32, V = 11.72, I = 8.36$; for a comparison, HH73 (in their numbering system the star is #9009)

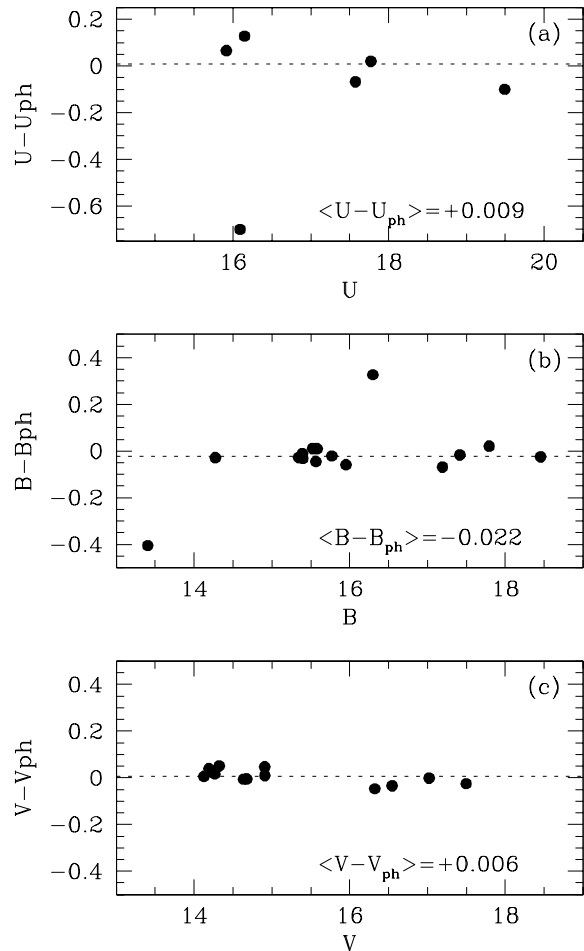


Figure 3. Comparison between our calibrated magnitudes and the photoelectric ones in HH73; also given are the mean differences (the zero points), computed excluding the more deviant measures (1 in U , 2 in B).

give $U = 19.59, B = 15.97,$ and $V = 11.68$. Since the star is variable, and so bright as to be near the saturation limit, we consider the magnitudes as acceptably similar. Taking into account the best values for distance modulus and reddening based on the synthetic colour-magnitude diagram method (Section 4), the absolute magnitude of the carbon star is $M_V = -1.90$ according to the Padova and FRANEC solar tracks and adopting $(m-M)_0 = 12.3$ and $E(B-V) = 0.41$, and in the range $-1.96 \leq M_V \leq -1.55$ according to the FST-ov models, where the higher uncertainty, due to the lack of He-burning phases, reflects in a range of equally acceptable distances and reddenings ($(m-M)_0 = 12.1-12.3$ and $E(B-V) = 0.37-0.43$). Stars in clusters or in binaries offer the best observational possibility of estimating the mass range where AGB evolution leads to the formation of carbon stars. In the case of NGC2660, all three best evolutionary models, even if they give different ages for the cluster, agree remarkably well on the mass presently at the TO: $2.0 M_\odot$ (FST) and $2.1 M_\odot$ (Padova and FRANEC). This represents a sharp lower limit to the mass of the carbon star, and is higher e.g., that the $1.8-1.9 M_\odot$ derived by Groenewegen et al. (1995).

3.1 Comparison with older data

We do not attempt any comparison with FDK: our data are not suitable for a variability search, since all frames were acquired in a short length of time (about 2.5 hours in the same night), and we have no better information on membership than the star positions on the CMD. We have counteridentified 11 stars, the three for which FDK show a light curve (their fig. 17), and a few more with parameter values indicating a variability larger than average. Their position on the CMD is as follows: $N_{\text{FDK}}=160$ ($N_{\text{our}}=589$), the spotted star, lies just above the MS, where binaries are found; $N_{\text{FDK}}=168$ ($N_{\text{our}}=392$) is possibly a field star; $N_{\text{FDK}}=459$ ($N_{\text{our}}=518$) is at the MS TO; six of the others (178/427, 381/311, 461/395, 555/389, 663/409, 717/205) are on the MS, one (417/536) is on the RGB, one (576/574) is in the Blue Stragglers region.

A more significant test is feasible with the HH73 data. We show in Fig. 2(d) their photographic $V, B - V$ diagram next to ours (Fig. 2(c)): our photometry clearly shows a smaller scatter and reaches a fainter magnitude limit.

HH73 used a set of photoelectric measurements to calibrate their data; we identified 15 of these stars in our field and compared our resulting magnitudes to their photoelectric values (Fig. 3), to test the validity of our calibration for the U, B, V filters. We found small offsets; the mean differences, once we removed the extreme deviant cases (possible misidentifications or image blends in our or in their photometry), are (our values minus HH73): 0.009 mag in U , -0.022 in B (the frame with the worst seeing and airmass), and 0.006 in V .

We decided to shift our values by those very small quantities, on the basis of the general superior quality of photoelectric magnitudes and of the intrinsic uncertainties on the extinction correction (the errors attached to the extinction coefficients translate to uncertainties of a few hundredths of magnitudes). Furthermore, when comparing the Zero Age Main Sequence (ZAMS) taken from Lang (1991) to our data in the two-colour diagram (see Fig. 4(a), we obtained a good fit with a reasonable value for the reddening $E(B - V) = 0.45$ (and $E(U - B) = 0.72 \times E(B - V)$, Cardelli, Clayton & Mathis 1984) only with the shifted data. This value for the reddening will be later compared to what is found from our CMD simulations. The comparison with this ZAMS cannot yield by itself the final value, since the cluster has an age large enough (see Sect. 4) to display evolutionary effects; furthermore, we would be assuming solar metallicity. Even if this seems to be a good enough approximation for NGC2660, the locus of populations of different metallicity in the two-colour diagram has not a simple dependence on metallicity (see e.g. Bressan, Granato & Silva 1998, their fig.8). The I values were of course left unaltered; in any case, the I band is the least affected by extinction.

The table with the photometry will be available through the CDS and BDA (Mermilliod 1995, maintained at <http://obswww.unige.ch/webda>).

3.2 Cluster members and binary sequence

We do not have any nearby external frame to estimate the degree of contamination by intervening field stars, but it

doesn't appear very important, especially in the red giant and clump region.

A possibility to discriminate between cluster members and field interlopers is given by the two-colours diagrams. Given the age of the cluster (around 1 Gyr), we are able to sample on the MS the spectral types $\sim A7-K2$ and fit our data to the ZAMS (Lang, 1991). We found a good fit using a reddening of $E(B - V) = 0.45$. We tried to isolate true MS members of the cluster selecting only stars falling on/near the locus defined by the MS stars in the two-colours diagrams, both in $B - V, U - B$ and $V - I, U - B$ (see Fig.4(a) and (b)). This could look like a somewhat arbitrary process, especially at fainter magnitudes, but it produces a reasonable CMD: see Fig.4(c), with 420 MS objects selected in the $B - V, U - B$ plane, and (d), with 399 objects selected in the $V - I, U - B$ plane. Red giants and clump objects, for a total of 34 stars, were all retained (they are represented in these figures by the open star symbols). Finally, we chose as "true cluster members" all the stars present in both selections (373 MS objects), plus the 34 giants, for a total of 407. This sample will be later compared to the simulated CMDs.

To determine an approximate fraction of binary stars we followed the same procedure already adopted for the other examined clusters. In this case, we used the $U, U - I$ diagram, since it offers the larger colour baseline, and made histograms in $U - I$ along the cluster MS (see Fig. 5, left panels). The more prominent peak corresponds to the main sequence; in the brighter magnitude interval, the second peak represents the red clump stars. Going fainter, a smaller secondary peak appears, that we attribute to the binaries: its position is in agreement with the colour that a sequence brighter than the MS by 0.75 mag (i.e. an equal-mass binary sequence) would have in each mag interval (see Fig. 5, right panel). Counting the stars in the two peaks, we determine an approximate fraction of 30% of binary stars. This fraction turns out to be in good agreement with that found necessary for the synthetic CMDs to well reproduce the observed one.

4 CLUSTER PARAMETERS

We derived the values of the cluster parameters applying to NGC2660 the usual approach of CMD simulations described by Tosi et al. (1991) and already employed in our previous works on open clusters. Due to the range of the existing estimates of the cluster metal content ($[\text{Fe}/\text{H}] \sim -1$ to slightly more than solar), the available stellar evolutionary tracks appropriate to create the synthetic CMDs are those with metallicities between solar and 1/5 of solar. As in our previous papers, to give an estimate of the uncertainty related to the theoretical interpretation of the CMD, we performed the simulations adopting several homogeneous sets of stellar models. The major features of these sets are summarized in Table 3. The FRANEC and Padova models adopt the standard mixing-length theory without and with overshooting from convective zones, respectively. In the FST models, instead, convection is treated following the Full Spectrum of Turbulence approach, with (FST-ov) and without (FST-st) overshooting. For each set of stellar models, we performed several MonteCarlo simulations for any reasonable combination of age, reddening and distance modulus.

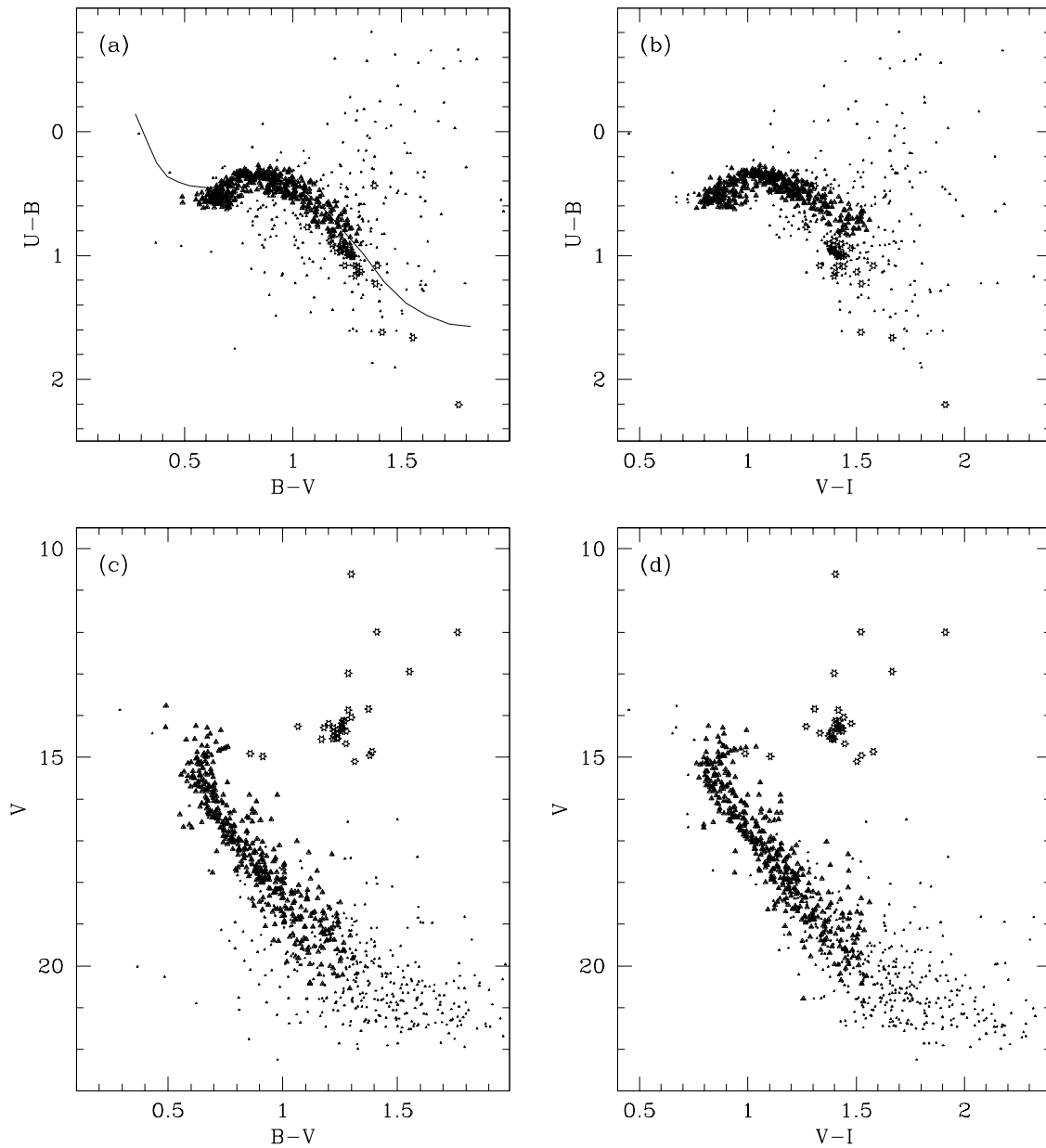


Figure 4. Selection of MS stars in the two-colours diagrams; in all panels filled triangles represent stars selected as cluster members on the MS, small points stand for stars rejected as members, and open stars represent the RGB/clump objects. (a) $V - B, U - B$ selection, with the ZAMS reddened by $E(B - V) = 0.45$; (b) $V - I, U - B$ selection. (c) and (d) show which stars were selected in the three groups in the $V, B - V$ and $V, V - I$ CMDs respectively.

To avoid spurious effects due to inhomogeneous conversions from the theoretical to the observational plane, all the model luminosities and temperatures have been transformed to magnitudes and colours using the same set of conversion tables, based on Bessel, Castelli & Plez (1998 a, b) model atmospheres.

The incompleteness factors and the photometric errors in each magnitude bin assigned to the synthetic stars in every photometric band are those derived from the observed data and mentioned in section 2. The number of stars in the synthetic diagram is 407, the same as that in the empirical CMDs shown in Fig.6 (top panels). The reddening $E(B -$

$V)$ is transformed to the $E(V - I)$ proper for our photometric bands following Taylor’s (1986) prescriptions.

4.1 Results with Padova stellar models

For these tracks we computed the synthetic CMDs with three different metallicities: $Z=0.02$, $Z=0.008$ and $Z=0.004$ (Bressan et al. 1993; Fagotto et al. 1994). Representative CMDs ($V, B - V$ on the left and $V, V - I$ on the right) derived from each of these sets of models are shown in Fig. 6. These synthetic CMDs assume that all the stars in NGC2660 are single.

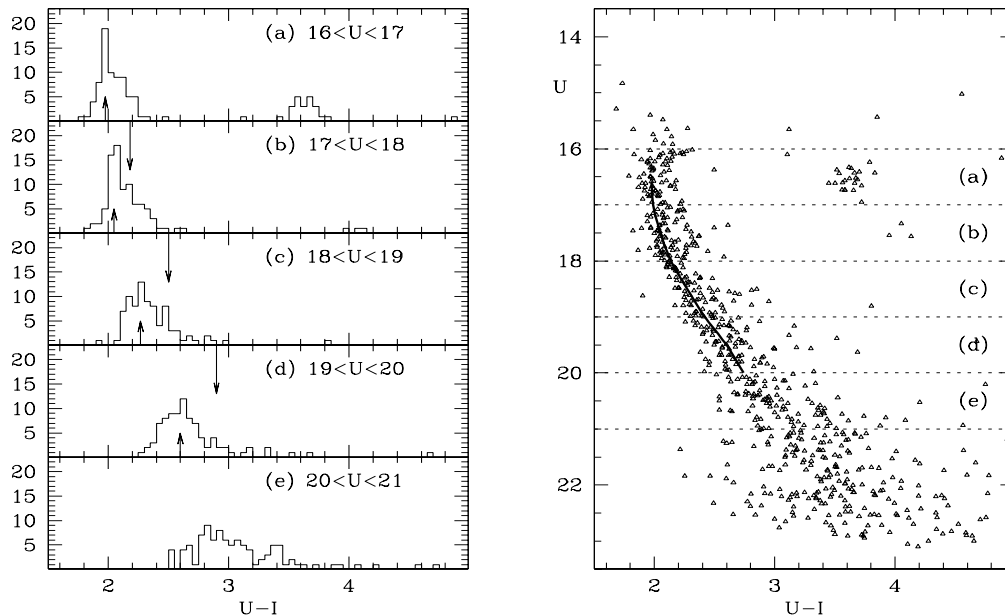


Figure 5. Histogram in colour at different magnitude levels along the cluster MS (left); the two arrows indicate the MS and the secondary peak. CMD of the cluster in $U, U - I$, with the adopted MS ridge line (right).

Table 3. Stellar evolutionary tracks adopted for the synthetic CMDs.

Model	Y	Z	M_{min} (M_{\odot})	M_{max} (M_{\odot})	Reference	Notes
FRANEC	0.28	0.02	0.7	9	Dominguez et al. 1999	to AGB-tip
FRANEC	0.27	0.01	0.7	9	private communication	to AGB-tip
FST-st	0.27	0.017	0.6	15	Ventura et al. 1998	to RGB-tip
FST-ov	0.27	0.017	0.6	15	Ventura et al. 1998	to RGB-tip
Padova	0.28	0.02	0.6	120	Bressan et al. 1993	to AGB-tip
Padova	0.25	0.008	0.6	120	Fagotto et al. 1994	to AGB-tip
Padova	0.24	0.004	0.6	120	Fagotto et al. 1994	to AGB-tip

The solar case corresponds to a cluster age of 950 Myr, $E(B - V) = 0.4$ and $(m-M)_0 = 12.3$. The $Z=0.008$ CMDs assume age = 1.1 Gyr, $E(B - V) = 0.52$ and $(m-M)_0 = 12.2$, and the $Z=0.004$ ones assume age = 1 Gyr, $E(B - V) = 0.56$ and $(m-M)_0 = 11.9$. These models were selected within each set as those with TO and clump stars luminosities and distributions in better agreement with the observed ones.

The MS gaps and the shape of MS, TO and post-MS phases are all very well reproduced by the $Z=0.02$, while the $Z=0.008$ models show a slightly shorter colour extension of the TO region and the metal poorer cases also show rounder TOs and different shapes of the MS, which worsen the fit to the data. Besides, while the reddening required for the solar models ($0.38 \leq E(B - V) \leq 0.42$) is consistent with the literature values (0.35 to 0.38, see Introduction) and with the one found for our data in the two-colour diagram (0.45), the reddening implied by the $Z=0.008$ models ($0.47 \leq E(B - V) \leq 0.52$) is barely acceptable, and that for the metal poorer models ($E(B - V) \geq 0.56$) is in our opinion too high. We thus suggest that the metallicity of NGC2660 is at least half solar.

4.2 Results with FRANEC stellar models

The FRANEC stellar tracks have been recently updated (Dominguez et al. 1999) to improve the input physics and include the OPAL opacities (Rogers, Swenson & Iglesias 1996). Thanks to their authors (Straniero, private communication), we have been able to use not only the published tracks but also others interpolated at intermediate metallicities. Given the worse results obtained with the lower metallicity set of Padova models, which apply also to the FRANEC cases, we present here only the FRANEC results for $Z=0.02$ and $Z=0.01$.

Both the solar and the half-solar metallicity models reproduce fairly well the detailed features visible in the observational $V, B - V$ and $V, V - I$ CMD (like bumps and gaps on the MS), when the adopted age is between 700 and 800 Myr. The colour extension of the TO region is however slightly short and a few subgiants are predicted where the cluster does not show them. The results are visible in the top and second panels of Fig. 7, where the CMDs of single stars with $Z=0.02$, age=750 Myr, $E(B - V) = 0.42$, $(m-M)_0 = 12.3$ and

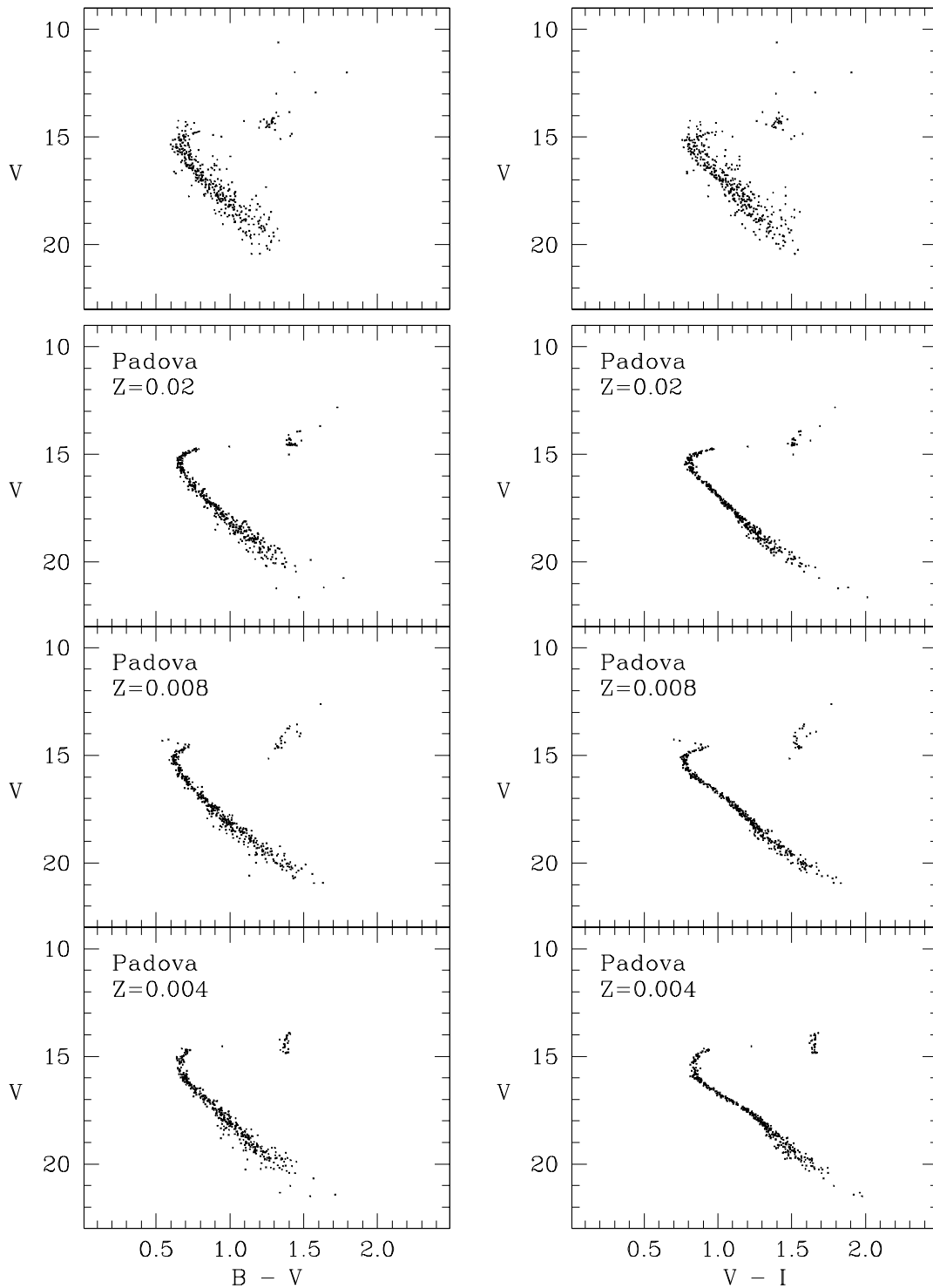


Figure 6. Reference observational CMDs of NGC2660 (top panels) and representative synthetic CMDs (single stars only) for the Padova sets of stellar tracks. The left panels show the $V, B - V$ diagrams and the right panels the $V, V - I$ ones. See text for details.

those for $Z=0.01$, age=700 Myr, $E(B - V) = 0.53$ and $(m - M)_0 = 12.2$ are shown, respectively. Older ages imply brighter clumps, different shapes of the MS and too round TOs, while younger ages imply fainter clumps and excessively hooked TOs. The same range of ages is found to best fit the data with both metallicities. Note that these ages are younger

than those obtained with the Padova models, as a direct consequence of the different assumption on overshooting from convective zones.

Of course, to reproduce the observed colours, the solar models require a lower reddening than the half-solar ones, because the latter are intrinsically bluer. In practice, the

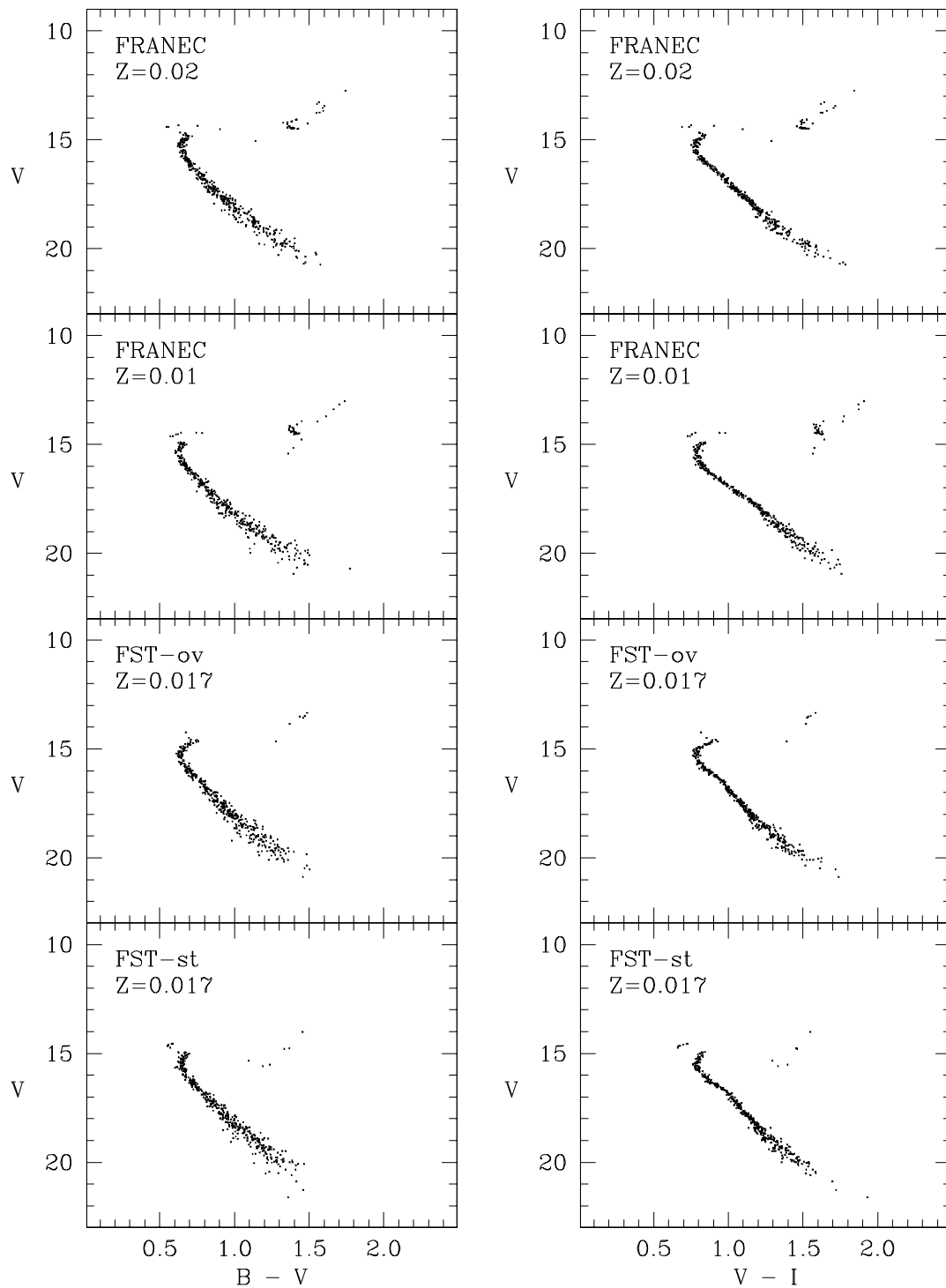


Figure 7. Same as Fig. 6 but for the FRANEC (upper panels) and FST (lower panels) stellar tracks.

synthetic CMDs in better agreement with the empirical one assume $E(B - V)$ around 0.5 when $Z=0.01$ and around 0.4 when $Z=0.02$. Bearing in mind the literature value and our fit in the two-colour diagram, we consider the above result as an indication that the metallicity of NGC2660 is more likely solar.

No significant difference is found in the distance modu-

lus with varying metallicity: with $Z=0.02$ the best CMDs adopt $(m-M)_0=12.3$, while with $Z=0.01$ they adopt $(m-M)_0=12.2$.

4.3 Results with FST stellar models

The FST models (Ventura et al. 1998) are available both with and without overshooting from convective zones, although only for solar metallicity. They thus allow for a direct test, in homogeneous conditions, of the effect of overshooting in the parameters derivation. Unfortunately, these tracks reach only the tip of the red giant branch and have no core helium burning phases. Hence they do not provide the extremely useful constraint represented by the clump features. For this reason, it is more difficult to limit the range of acceptable ages with these tracks. In fact, with the FST-st models any age between 700 Myr and 1 Gyr seems acceptable, whereas with the FST-ov models the range moves toward older values (0.9–1.2 Gyr) as a classical consequence of overshooting.

Another effect of the higher luminosity related to the overshooting assumption is the higher reddening required to reproduce the observed colours. For the same age (and, obviously, metallicity), the FST-ov models have to assume $E(B - V)$ at least 0.03 higher than the corresponding FST-st models. However, when the age is allowed to vary and its best range is selected, the older age required by overshooting models makes the synthetic CMDs redder and somewhat compensates the reddening difference. As a consequence, the reddenings resulting in the two cases are fairly similar to each other: overshooting models indicate $E(B - V)$ between 0.37 and 0.43, and standard models $E(B - V)$ between 0.38 and 0.48.

The most striking characteristics of the FST-ov models is that the observed features of the MS, TO and sub-giant regions are incredibly well reproduced, even the smallest gaps or shapes which one would have not considered as significant. The FST-st models also reproduce well the MS features but to a less extent. The quality of the fit can be appreciated in the bottom and second from bottom panels of Fig. 7, where we show the synthetic CMDs for single stars corresponding to the FST-ov case with age 1.1 Gyr, $E(B - V) = 0.37$ and $(m-M)_0 = 12.1$ and to the FST-st case with age 900 Myr, $E(B - V) = 0.40$ and $(m-M)_0 = 12.3$.

4.4 The need for binary stars.

All the models in Figs 6 and 7 share the characteristics of presenting MS bands much tighter than the empirical one. One might think that this inconsistency comes from having underestimated the photometric errors, but this cannot be the case, at least for the brightest magnitude bin of the TO region, where the photometry is very accurate, the uncertainties very small, but the spread difference between data and predictions possibly larger than at fainter magnitudes. The obvious explanation for such difference resides in the presence of a significant fraction of binary stars.

In all the clusters already examined by our group (NGC2243, NGC2506, NGC6253, NGC7790, Be21 and Cr261) we found evidence for a significant fraction (30% at least) of binary stars. In NGC2660 the observational evidence is possibly less compelling, as discussed in Section 3.2, but the comparison between empirical and synthetic CMDs shows that binaries must be present in this cluster as well. Fig. 8 shows some of the best synthetic $V, B - V$ CMDs resulting from the various sets of stellar evolutionary models,

together with their luminosity function (LF) overimposed to the empirical one. The only difference with respect to the models presented in Figs 6 and 7 is that 136 of the 407 stars are now supposed to be in binary systems with random mass ratios; their magnitudes and colours are thus modified according to Maeder's (1974) prescriptions for systems of any mass ratio between primary and secondary star.

It is apparent from Fig. 8 that the inclusion of this 30% of binaries allows us to perfectly reproduce the observed spread of the stellar distribution in all the CMD sequences, as well as the single morphological features of the distributions (gaps, hooks, bumps, etc.). The observational luminosity function is also quite well reproduced by these models, except in the FST cases, where the lack of the clump obviously reflects in a paucity of bright stars.

5 DISCUSSION AND CONCLUSIONS

All the models presented above turn out to show RGB colours redder than observed. We do not have a straight explanation for this problem, but we envisage three possible reasons: it can be related to a) an intrinsically too cool temperature of the stellar models, b) an inappropriate temperature–colour transformation in the coolest phases, c) an inappropriate application of the reddening law. The former two options cannot be excluded, but sound rather unlikely, since the problem equally affects all the stellar tracks examined so far and is found to be the same with any of the photometric conversions applied by our group. The latter explanation seems instead quite possible, because we applied to all the synthetic stars a constant $E(B - V)$ (i.e. independent of spectral type), whereas Twarog, Ashman & Anthony-Twarog (1997) have recently emphasized that stars of the RGB types show $E(B - V)$ lower by 5–10 % than that of MS stars with intrinsic $B - V$ 1.0 mag bluer. Fernie (1963) derived from a sample of supergiants the relation $E(B - V)_{true} = E(B - V) \times [0.97 - 0.09 \times (B - V)]$, which was later found by Hartwick & Hesser (1972) to hold also for red giants in open clusters. We have applied this relation to our synthetic CMDs and found that it does reduce, but not sufficiently, the excessive redness of our RGB stars. Since we have found no recent quantitative confirmation of the above relation, we have preferred to avoid introducing further uncertainties. Hence, all the synthetic diagrams shown here have been treated with a constant reddening.

We determined for NGC2660 a confidence interval for metallicity, distance, reddening and age: metallicity about solar, $(m-M)_0 = 12.1-12.3$, $E(B - V) = 0.37-0.42$, age $\lesssim 1$ Gyr, with a fraction of binaries of about 30 %.

The cases resulting in better agreement with the data are listed in Table 4 where they are ranked according to the fit quality. The ranking is the result of a quantitative comparison of the predicted LFs with the corresponding data and of independent selections by eye of the CMDs made by each of the authors. Such ranking is in agreement with what can be derived from χ^2 or Kolmogorov-Smirnov tests. Nonetheless, given the uncertainties still affecting the synthetic CMDs for the problems mentioned at the beginning of this section, statistical tests cannot help much in discriminating among the models and we believe that a better

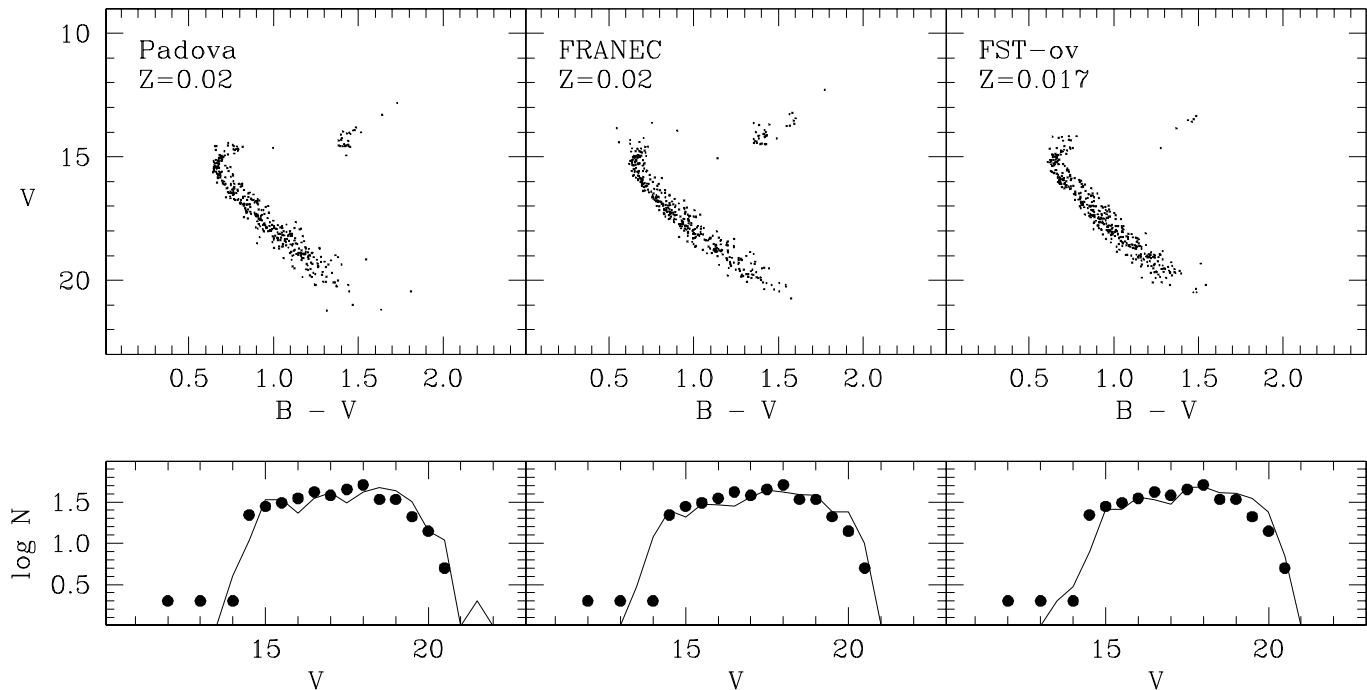


Figure 8. Best synthetic CMDs with 30% of binary stars for each group of stellar models. The top panels show the $V, B - V$ diagrams and the bottom panels the corresponding LF (solid line) overimposed on the empirical one (dots). See text for further details.

Table 4. Summary of best-fitting results for distance modulus, age, and reddening, chosen from all the simulations.

Model	Z	(m-M) ₀	τ (Gyr)	$E(B - V)$	Notes
Padova	0.02	12.3	0.95	0.40	
FRANEC	0.02	12.3	0.75	0.42	
FST-ov	0.017	12.1	1.10	0.37	ages ≥ 0.9 Gyr acceptable
Padova	0.02	12.3	1.00	0.38	
FST-ov	0.017	12.1	1.20	0.37	ages ≥ 0.9 Gyr acceptable
FRANEC	0.01	12.2	0.70	0.55	

selection can still be achieved by eye, which allows to take such uncertainties more easily into account.

We recall, once again, that the FST models have generally lower ranks because they lack the He-burning phases (i.e. the clump) and despite their better fit in the computed phases. Given the method used, the parameters attributed to the cluster are strictly tied, and changing one of them implies changing them all. The quality of the fits, though, is so good, that each parameter has only a very limited possible range.

All the best fits are obtained for solar metallicity; furthermore, the high reddenings implied by the more metal poor tracks are in contradiction both with what we find from our two-colours diagram, and with literature values based on different methods. Our best estimate of the metallicity, based on our photometry, is in reasonable agreement with HH73, and Lyngå (1987). The vastly different values found in literature cannot be reconciled: the best way out of the

problem is, of course, through high resolution spectroscopic analysis.

The distance moduli resulting from the synthetic diagrams vary between 11.9 and 12.5, but the extremes produce significantly worse fits, and for all the good reproductions of the observed CMD, the distance modulus values cluster around 12.2.

The age seems to be the parameter less well determined, but the difference is mostly between models with and without overshooting: the FRANEC evolutionary tracks give ages consistently lower than the Padova or FST-ov ones. About the latter, the lack of the red clump phase implies that the age can not be very well constrained: in fact, both the 900 Myr and the 1 Gyr models match the observed CMD as well as the 1.1 and 1.2 Gyr ones, without significant variations of all other parameters.

Finally, we want to stress the fact that, when all the other parameters are the same, models including overshooting from the convective zones seem to better reproduce the

observed data. We were able to test it by direct comparison of models computed by the same authors (Ventura et al. 1998), using exactly the same inputs and codes, except for the presence/absence of overshooting. The validity of this important test would be greatly enhanced by the availability of a set of tracks complete of all evolutionary phases.

ACKNOWLEDGEMENTS

We warmly thank P. Montegriffo, for his expert assistance with data reduction. We are grateful to A. Chieffi, M. Limongi and O. Straniero for the new unpublished FRANEC tracks and for the table for photometric conversions. P. Ventura has also kindly provided the FST tracks in appropriate format. The bulk of the numerical code for CMD simulations has been provided by Laura Greggio. S.S. has been partially funded on the ASI contract ARS-96-70. This research has made use of the Simbad database, operated at CDS, Strasbourg, France and of the BDA database, maintained by J.C. Mermilliod. We thank J.C. Mermilliod also for his careful referee report, which has allowed us to significantly improve the paper presentation.

REFERENCES

- Bessel, M.S., Castelli, F., Plez, B. 1998, *A&A*, 333, 231
 Bessel, M.S., Castelli, F., Plez, B. 1998, *A&A*, 337, 321
 Bonifazi, A., Fusi Pecci, F., Romeo, G., Tosi, M. 1990, *MNRAS*, 245, 15
 Bragaglia, A., Tessicini, G., Tosi, M., Marconi, G., Munari, U. 1997, *MNRAS*, 284, 477
 Bressan, A., Fagotto, F., Bertelli, G., Chiosi, C. 1993, *A&AS*, 100, 647
 Bressan, A., Granato, G.L., Silva, L. 1998, *A&A*, 332, 135
 Cardelli, J.A., Clayton, G.C., Mathis, J.S. 1984, *ApJ*, 345, 245
 Carraro, G., Chiosi, C. 1994, *A&A*, 287, 761
 Carraro, G., Ng, Y.K., Portinari, L. 1998, *MNRAS*, 296, 1045
 Dominguez, I., Chieffi, A., Limongi, M., Straniero, O. 1999, *ApJ*, in press, astro-ph/9906030
 Fagotto, F., Bressan, A., Bertelli, G., Chiosi, C. 1994, *A&AS*, 105, 29
 Fernie, J.D. 1963, *AJ*, 68, 780
 Frandsen, S., Dreyer, P., Kjeldsen, H. 1989, *A&A*, 215, 287 (FDK)
 Friel, E.D. 1995, *ARA&A*, 33, 381
 Geisler, D., Clariá, J.J., Minniti, D. 1992, *AJ*, 104, 1892
 Gozzoli, E., Tosi, M., Marconi, G., Bragaglia, A. 1996, *MNRAS*, 283, 66
 Greggio, L., Tosi, M., Clampin, M., DeMarchi, G., Leitherer, C., Nota, A., Sirianni, M. 1998, *ApJ*, 504, 725
 Groenewegen, M.A.T., van den Hoeck, L.B., de Jong, T. 1995, *A&A*, 293, 381
 Janes, K.A., Phelps, R.L. 1994, *AJ*, 108, 1773
 Hartwick, F.D.A., Hesser, J.E. 1973, *ApJ*, 183, 883 (HH73)
 Hartwick, F.D.A., McClure, R.D. 1972, *PASP*, 84, 288
 Hesser, J.E., Smith, G.H. 1987, *PASP*, 99, 1044
 Houdashelt, M.L., Frogel, J.A., Cohen, J.G. 1992, *AJ*, 103, 163
 Landolt, A.U. 1992, *AJ*, 104, 340
 Lang, K.R. 1991, *Astrophysical Data*, Springer-Verlag, p. 149
 Lewis, J.R., Freeman, K.C. 1989, *AJ*, 97, 139
 Lyngå, G. 1987, *Catalogue of Open Cluster Data* (5th ed.), Lund Observatory, distributed by CDS
 Maeder, A., 1974, *A&A*, 32, 177
 Marconi, G., Hamilton, D., Tosi, M., Bragaglia, A. 1997, *MNRAS*, 291, 763
 Mermilliod, J.C. 1995, D. Egret, M.A. Albrecht eds, *Information and On-Line Data in Astronomy*, Kluwer Academic Press (Dordrecht), p. 127
 Piatti, A.E., Clariá, J.J., Abadi, M.G. 1995, *AJ*, 110, 2813
 Rogers, F.J., Swenson, F.J., Iglesias, C.A. 1996, *ApJ*, 456, 902
 Romeo, G., Bonifazi, A., Fusi Pecci, F., Tosi, M. 1989, *MNRAS*, 240, 459
 Stetson, P.B. 1992, *User's Manual for DAOPHOT-II*
 Taylor, B.J. 1986, *ApJS*, 60, 577
 Tosi, M., Greggio, L., Marconi, G., Focardi, P. 1991, *AJ*, 102, 951
 Tosi, M., Pulone, L., Marconi, G., Bragaglia, A. 1998, *MNRAS*, 299, 834
 Twarog, B.A., Ashman, K.M., Anthony-Twarog, B.J. 1997, *AJ*, 114, 2556
 Ventura, P., Zeppleri, A., Mazzitelli, I., D'Antona, F. 1988, *A&A*, 334, 953